Tunable band gap in twisted bilayer graphene

Xiu-Cai Jiang,* Yi-Yuan Zhao,* and Yu-Zhong Zhang†

Shanghai Key Laboratory of Special Artificial Microstructure Materials and Technology, School of Physics Science and Engineering, Tongji University, Shanghai 200092, People's Republic of China

(Received 16 December 2021; accepted 23 February 2022; published 4 March 2022)

At large commensurate angles, twisted bilayer graphene which holds even parity under sublattice exchange exhibits a tiny gap. Here, we point out a way to tune this tiny gap into a large gap. We start from comprehensive understanding of the physical origin of gap opening by density functional theory calculations. We reveal that the effective interlayer hopping, intralayer charge-density wave, or interlayer charge imbalance favors a gap. Then, on the basis of tight-binding calculations, we suggest that a periodic transverse inhomogeneous pressure, which can tune interlayer hoppings in specific regions of the moiŕe supercell, may open a gap of over 100 meV, which is further confirmed by first-principles calculations. Our results provide a theoretical guidance for experiments to open a large gap in twisted bilayer graphene.

DOI: 10.1103/PhysRevB.105.115106

I. INTRODUCTION

Electronic properties of twisted bilayer graphene (tBLG) [1] are strongly affected by moiŕe pattern and interlayer coupling [2]. As a result, many exotic phenomena, such as a Mott insulator [3,4], superconductivity [5–7], and a higher-order topological insulator [8,9] have been discovered in tBLG with different stacking configurations. Of particular interest, at large commensurate angles, tBLG, which holds even parity under sublattice exchange (SE), has not only graphene-like low-energy spectra [10,11], but also an intrinsic gap at half-filling [11,12], making it a promising candidate for high-mobility field effect transistors. However, the gap is too small to switch off electrical conduction at room temperature, which impedes such applications [13].

Therefore, in order to overcome this problem, much effort has been made to investigate conditions for gap opening at half-filling and properties of gapped states. It was proposed that the ground state of the tBLG with twisted angle $\theta = 38.21^\circ$ is insulating with an intrinsic gap of less than 10 meV at half-filling over a decade ago [11]. Using a long-wavelength theory, Mele pointed out that all SE-even structures are gapped, which are ascribed to pseudo-spin-orbit coupling resulting from hoppings between layers [14,15]. From the tight-binding analyses, it was shown that gaps only exist in SE-even tBLG with a twisted angle $\theta > \theta_c \approx 1.89^\circ$ [16]. Thus, the gap can be tuned by twisting different angles between two layers. Besides, in-plane strains can tune the gap as well where a direct-indirect gap transition occurs under mixed in-plane strains [17]. Moreover, recently, SE-even structures with large twisted angles were proposed to be higher-order topological insulators hosting corner states which emerge as long as the underlying symmetries are intact [8]. These findings further trigger the interest to study the gapped state in SE-even tBLG.

However, until now, despite extensive investigations, an effective way to open a large gap in SE-even tBLG has not yet been proposed. In fact, if only twisting is employed between layers, the gap is so small that one needs to control the twisted angle accurately in a clean sample to observe it at low temperature [18]. Fortunately, the twisted angle can be controlled with a remarkable precision of 0.1° in experiments [19–21]. Besides, the techniques to compress the interlayer distance down to 80% [22] to exert an in-plane tensile strain up to 6% without inelastic relaxation [23] and to apply a transverse electric field [24] have been mastered. Applying these techniques to tBLG can lead to many novel phenomena, such as pressure dependence of flat bands [25–27], magnetism induced by pressure at a large twisted angle [27], direct-indirect gap transition induced by mixed in-plane strains [17], and a tunable gap induced by a transverse electric field [24]. Furthermore, tBLG has intralayer on-site potential differences [28], which are neglected in long-wavelength theory [14] and tight-binding approximation [16]. On-site potential differences in the layer often induce an in-plane uneven charge distribution resulting in an intralayer charge-density wave (CDW), which may affect the gap. Hence, clarifying the effect of the CDW on gap opening and finding a way to open a large gap in tBLG with above available techniques are topical subjects.

In this paper, we point out a way to tune the tiny gap of tBLG with twisted angle $\theta = 38.21^\circ$ into a large gap. First, to show the tunable properties of gap, using first-principle calculations, we study the effects of external tuning parameters, such as a transverse homogeneous pressure, an in-plane biaxial tensile strain, or a transverse electric field on gap opening. We find that the gap increases monotonously with increasing these tuning parameters. Second, to understand the reasons why the gap increases with these parameters, we calculate effective interlayer hopping and order parameters

*These authors contributed equally to this work.
†Corresponding author: yzzhang@tongji.edu.cn

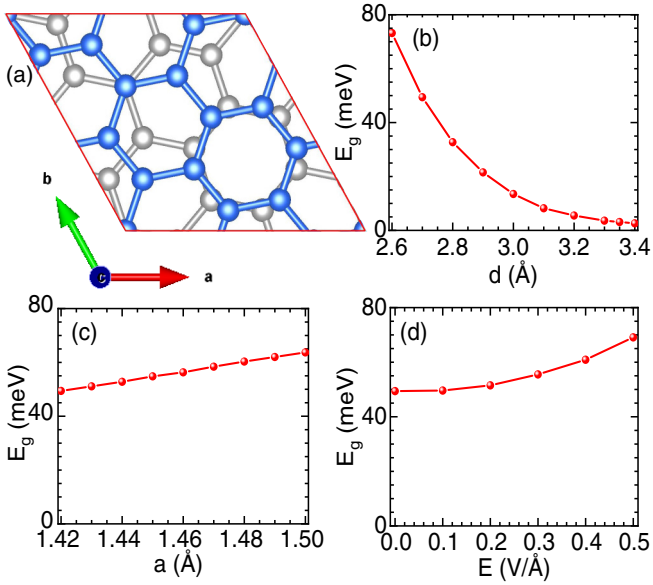

FIG. 1. (a) The structure of SE-even tBLG with twisted angle $\theta = 38.213^\circ$. (b) The gap as a function of d, where $a = 1.42$ Å is used. (c) The gap as a function of a, where $d = 2.7$ Å is adopted. (d) The gap as a function of gated field E, where $a = 1.42$ Å and $d = 2.7$ Å are used.

of intra- and interlayer charge disproportionations. We reveal that enhancement of gap amplitude with applying pressures or strains is attributed to the increase in both intralayer CDW and effective interlayer hopping where the latter always plays a dominant role on gap opening, whereas the external electric field can induce an interlayer charge imbalance, resulting in enlargement of the gap. Third, using the tight-binding model, we demonstrate how to open a larger gap by tuning interlayer hoppings and on-site potentials which can modify intralayer CDW in specific regions of the moiŕe supercell, respectively. Finally, based on the guidance of tight-binding calculations, we suggest that a periodic transverse inhomogeneous pressure can open a gap of over 100 meV, which is further confirmed by first-principle calculations.

Our paper is organized as follows. Section II describes the details of the structure, the model, and the method we used. Section III presents our main results, including gaps as functions of different external tuning parameters, density of state (DOS) and band structures, contour maps of the difference in charge density, effective interlayer hopping and order parameters of CDW states, analyses of tight-binding calculations, and variations of different physical quantities as functions of effective periodic transverse inhomogeneous pressure. Section IV includes a discussion of our results, and Sec. V concludes with a summary.

II. MODEL AND METHOD

The structure of tBLG with twisted angle $\theta = 38.21^\circ$, which can be realized in experiment [29], is shown in Fig. 1(a). According to the atomic environment, we identify three distinct regions in the moiŕe supercell, namely, A, H, and M regions as shown in Fig. 5(a), corresponding to the region where atoms of two layers (green) sits on top of each other, the region where hexagon centers of two layers overlap (pink), and the region of the rest (blue), respectively.

To calculate the properties of tBLG under a transverse homogeneous pressure, an in-plane biaxial tensile strain, a transverse electric field, or a periodic transverse inhomogeneous pressure, density functional theory (DFT) calculations are employed, based on the projector augmented-wave method [30] as implemented in the Vienna *ab initio* simulation package [31,32]. We choose the generalized gradient approximation of Perdew-Burke-Ernzerhof [33] to the exchange-correlation potentials with van der Waals correction called vdW-DF2-B86r [34,35], which is considered to be the functional with the best overall performance in multilayer graphene [36]. A plane-wave energy cutoff of 450 eV is employed. A Γ-centered K-point grid of $45\times45\times1$ is used in the Brillouin-zone integral. The vacuum distance is set to be 20 Å to eliminate the coupling between periodic images of the layers in the direction perpendicular to the atomic planes.

To demonstrate how to open a large gap by tuning interlayer hoppings and on-site potentials in distinct regions of the moiŕe supercell, a simple model is introduced as

$$H = H_D + \delta H_t + \delta H_\Delta, \tag{1}$$

where

$$H_D = \sum_{is\sigma} \Delta_{is} C^\dagger_{is\sigma} C_{is\sigma} - \sum_{is\sigma} \sum_{js'}{}' t_{isjs'} C^\dagger_{is\sigma} C_{js'\sigma} \tag{2}$$

is the Hamiltonian derived from DFT calculations with tight-binding parameters obtained through transformation from the Bloch space to the maximally localized Wannier function basis by using the WANNIER90 code [37,38]. Totally, 28 bands close to the Fermi energy are taken into account for each spin, which are mainly contributed from p_z orbitals of 28 carbon atoms in the moiŕe supercell. δH_t and δH_Δ are perturbed Hamiltonians that can be viewed as modeling of external perturbations, such as applying pressures, strains, and electric fields which result in interlayer hoppings or on-site potentials deviating from their DFT values. Here, δH_t contains five terms whereas δH_Δ includes three terms,

$$\begin{aligned} \delta H_t &= \delta H_{t_A} + \delta H_{t^1_M} + \delta H_{t^2_M} + \delta H_{t^1_H} + \delta H_{t^2_H}, \\ \delta H_\Delta &= \delta H_{\Delta_A} + \delta H_{\Delta_M} + \delta H_{\Delta_H}, \end{aligned} \tag{3}$$

where

$$\begin{aligned} \delta H_{t_A} &= \delta t_A \sum_{i\sigma} \sum_{\langle s,s'\rangle \in A} C^\dagger_{is\sigma} C_{is'\sigma}, \\ \delta H_{t^1_M} &= \delta t^1_M \sum_{i\sigma} \sum_{\langle s,s'\rangle \in M} C^\dagger_{is\sigma} C_{is'\sigma}, \\ \delta H_{t^2_M} &= \delta t^2_M \sum_{i\sigma} \sum_{\langle\langle s,s'\rangle\rangle \in M} C^\dagger_{is\sigma} C_{is'\sigma}, \\ \delta H_{t^1_H} &= \delta t^1_H \sum_{i\sigma} \sum_{\langle s,s'\rangle \in H} C^\dagger_{is\sigma} C_{is'\sigma}, \\ \delta H_{t^2_H} &= \delta t^2_H \sum_{i\sigma} \sum_{\langle\langle s,s'\rangle\rangle \in H} C^\dagger_{is\sigma} C_{is'\sigma}, \end{aligned}$$

$$\delta H_{\Delta_A} = \delta\Delta_A \sum_{i\sigma}\sum_{s\in A} C^{\dagger}_{is\sigma} C_{is\sigma},$$
$$\delta H_{\Delta_M} = \delta\Delta_M \sum_{i\sigma}\sum_{s\in M} C^{\dagger}_{is\sigma} C_{is\sigma},$$
$$\delta H_{\Delta_H} = \delta\Delta_H \sum_{i\sigma}\sum_{s\in H} C^{\dagger}_{is\sigma} C_{is\sigma}. \quad (4)$$

Here, i (j), s (s'), and σ denote cell, sublattice, and spin index, respectively. $\langle s, s'\rangle$ ($\langle\langle s, s'\rangle\rangle$) means the summation over interlayer nearest (next-nearest)-neighbor sites. δt_A, δt_M^1, δt_M^2, δt_H^1, and δt_H^2 are the deviations of interlayer hopping integrals in corresponding regions [see Fig. 5(a)] from their DFT values due to external perturbations, whereas $\delta\Delta_A$, $\delta\Delta_M$, and $\delta\Delta_H$ stand for the deviations of on-site potentials in corresponding regions from their DFT values. Thus, using this model, we can study the effect of external perturbations, which affect interlayer hoppings or on-site potentials in distinct regions of the moiŕe supercell, on gap opening.

III. RESULTS

Now, we start with the tunable properties of the gap in SE-even tBLG with twisted angle of $\theta = 38.21^\circ$. Figure 1(b) shows the gap as a function of interlayer distance d, where intralayer C-C bond length $a = 1.42$ Å is adopted. As can be seen, the system is always gapped despite the differences in the interlayer distance. The gap increases monotonously with a decrease in d, which can be effectively viewed as applying transverse homogeneous pressure. We estimate the magnitude of the pressure to be 30 GPa when $d = 2.7$ Å. Therefore, the gap of the system is tunable by a transverse homogeneous pressure. It is worth noting that gap of the equilibrium geometry of tBLG is of 3.1 meV, which is comparable with the results obtained from other first-principle calculations [11] and long-wavelength theory [14], but is not coincident with the result of tight-binding approximation where the unreasonable large gap was obtained [16]. Band gap opening is further confirmed by DOS and band structures as presented in Fig. 2(a) ($d = 2.7$ Å only) and Fig. 2(b), respectively.

To show the effect of an in-plane biaxial tensile strain on the gap opening of the system, we have calculated the gap as a function of intralayer C-C bond length a as shown in Fig. 1(c), where $d = 2.7$ Å is used. We find the gap increasing monotonously with the increase in a, indicating that gap increases monotonously with an applied in-plane biaxial tensile strain. The same conclusion is obtained by other first-principle calculations when the interlayer distance is fixed at the equilibrium distance [17]. The band-gap opening is further confirmed by band structures as illustrated in Fig. 2(c). Therefore, the gap is tunable by an in-plane biaxial tensile strain. A transverse electric field can induce symmetry breaking between top and bottom layers, which may tune the gap of the system. Figure 1(d) shows the gap as a function of a transverse electric field, where $a = 1.42$ and $d = 2.7$ Å are used. We find that the gap of the system increases monotonously with an applied transverse electric field, which is consistent with the results observed in experiment [24] and that obtained by the tight-binding model [39], but is contrary to the conclusion obtained by continuum approximation where the gapless

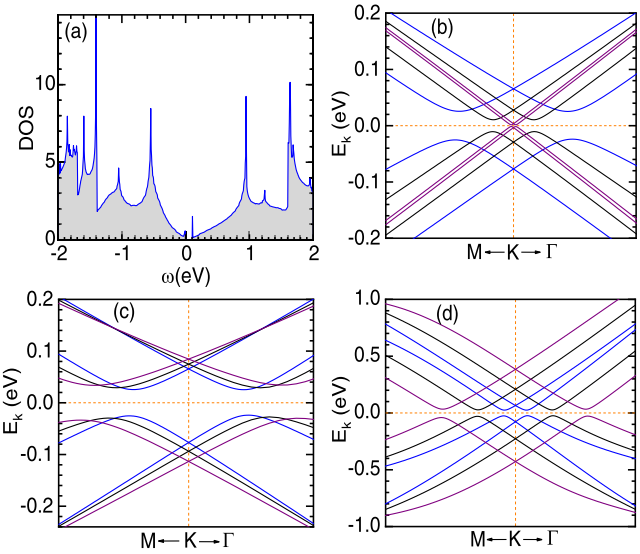

FIG. 2. (a) Total density of states for $a = 1.42$, $d = 2.7$ Å. (b) Band structures for different interlayer distances with 2.7 Å (blue), 2.9 Å (black), and 3.35 Å (purple), where $a = 1.42$ Å is used. (c) Band structures for different bond lengths with 1.42 Å (blue), 1.46 Å (black), and 1.50 Å (purple), where $d = 2.7$ Å is adopted. (d) Band structures for different gated fields with 0.0 V/Å (blue), 0.2 V/Å (black), and 0.4 V/Å (purple), where $a = 1.42$ and $d = 2.7$ Å are used.

state remains in the presence of the gated electric field [40]. Band structures under different transverse electric fields are presented in Fig. 2(d). Thus, an electric field can tune the gap as well.

It is worth noting that an intrinsic intralayer CDW exists in the system, which has not yet been mentioned. Besides, an interlayer charge imbalance occurs when applying a transverse electric field. To illustrate this, we show the contour maps of the charge-density difference between tBLG and superposition of two individual graphene layers where charges are equally distributed at all sites for different structures in Fig. 3. Interestingly, there is an uneven charge distribution in tBLG even with the structure of equilibrium geometry as shown in Fig. 3(a), indicating the existence of an intrinsic intralayer CDW. As we can see from Figs. 3(b) and 3(c), the uneven charge distribution enhances when applying a transverse homogeneous pressure and an in-plane biaxial tensile strain, respectively. Furthermore, when applying a transverse electric field, Fig. 3(d) exhibits an additional imbalance of charge distribution between top (blue) and bottom (gray) layers compared with the case without an electric field [Fig. 3(b)], indicating the formation of an interlayer charge imbalance. In fact, an intralayer CDW or an interlayer charge imbalance plays a crucial role in gap opening. Therefore, clarifying the effect of interlayer hoppings, intralayer CDW, and interlayer charge imbalance on gap opening is the key to obtain a larger gap in tBLG.

Next, we proceed to demonstrate that the gap size increasing with reduced interlayer distance or strengthened in-plane biaxial tensile strain is attributed to the increase in both intralayer CDW and effective interlayer hopping where the latter

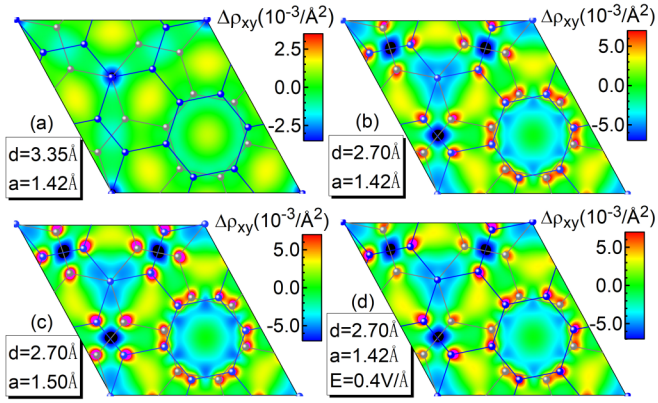

FIG. 3. Contour maps of charge-density difference between tBLG and superposition of two individual graphene layers for different structures with $d = 3.35, a = 1.42$ Å in (a), $d = 2.70$, $a = 1.42$ Å in (b), $d = 2.70, a = 1.50$ Å in (c), and $d = 2.70$, $a = 1.42$ Å, $E = 0.4$ V/Å in (d), respectively. Note that the scale of the color bar in (a) is half of that in (b)–(d).

always dominates gap opening, whereas the gap is enlarged by the gated electric field due to the formation of an interlayer charge imbalance.

A transverse homogeneous pressure can push the top and bottom layers closer together, which enhances both interlayer hybridizations and Coulomb interactions, leading to the increase in effective interlayer hopping and intralayer CDW. In order to quantify the strength of interlayer hoppings and intralayer CDW, we have calculated effective interlayer hopping t_{eff}, defined as the band splitting at the K point of Brillouin zone in the absence of intralayer CDW, and order parameter of the intralayer CDW $\Delta n_t = \sum_s |n_s - 1.0|$ as functions of d in Fig. 4(a), where $\sum_s$ sums over the sublattices in the supercell. Obviously, t_{eff} and Δn_t increase monotonously with reduced interlayer distance. As a result, both the gap induced by effective interlayer hopping alone E_g^{NCDW} where the effect of intralayer CDW is removed artificially, and the gap caused by intralayer CDW $E_g - E_g^{NCDW}$ (gray shadow) increase with the transverse homogeneous pressure as shown in Fig. 4(d). Thus, the real gap of the system E_g increases monotonously with the transverse homogeneous pressure. Moreover, one can see that the effective interlayer hopping dominates the gap opening.

An in-plane biaxial tensile strain stretches the in-plane C-C bond a, resulting in the decrease in intralayer hybridizations, indicating that p_z electrons around the C atoms are more localized in the intralayer direction whereas more extended in the interlayer direction. As a result, the effective interlayer hopping increases due to the increased overlap between wave functions of two layers, and the intralayer CDW is enhanced since electrons are more localized in the intralayer direction, which are confirmed by our calculations on effective interlayer hopping t_{eff} and order parameter of the intralayer CDW Δn_t as functions of a in Fig. 4(b). Therefore, through a similar analysis as we did in the case of applying transverse homogeneous pressure, we reveal that the E_g increasing monotonously with the in-plane biaxial tensile strain as shown in Fig. 4(e), can be ascribed to the increase in both intralayer CDW and

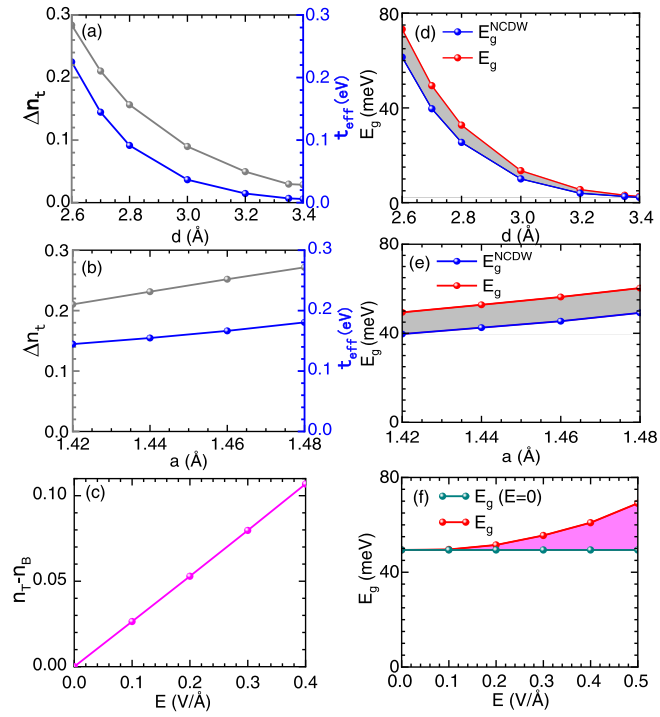

FIG. 4. (a) and (b) show the effective interlayer hopping t_{eff} and order parameter of the intralayer CDW Δn_t as functions of d and a, respectively. (c) Order parameter of the interlayer charge imbalance n_T-n_B as a function of E. (d) and (e) present E_g^{NCDW} and E_g as functions of d and a, respectively. E_g^{NCDW} is the gap induced by interlayer hoppings alone where the effect of intralayer CDW is removed artificially, whereas E_g is the real gap of the system. NCDW is the abbreviation of no charge-density wave. (f) E_g as a function of E, where $E_g(E = 0)$ is the gap without electric field. $a = 1.42$ Å is used in (a) and (d), $d = 2.70$ Å is used in (b) and (e), $d = 2.70$ and $a = 1.42$ Å are used in (c) and (f). The calculation method of t_{eff} for different structures are shown in Fig. 7 in Appendix A and Fig. 8 in Appendix B.

effective interlayer hopping where the latter always dominates the gap opening.

An (downward) electric field perpendicular to tBLG layers generates an electric potential difference between the top and the bottom layers, which leads to electronic charge transfer from the bottom to the top layers. We have calculated order parameter of interlayer charge imbalance $n_T - n_B = \sum_s^T n_s - \sum_{s'}^B n_{s'}$ as a function of E in Fig. 4(c), where $\sum_s^T$ and $\sum_{s'}^B$ sum over the sublattices of top and bottom layers in the supercell, respectively. We find that $n_T - n_B$ increases monotonously with the electric field. As a result, the gap is further opened as shown in Fig. 4(f), where $E_g - E_g(E = 0)$ (pink shadow) is the gap induced by the interlayer charge imbalance. Therefore, we reveal that gap increasing with the electric field is due to the formation of an interlayer charge imbalance.

In brief, gap of the system is tunable by interlayer distance, in-plane biaxial strain, and gated electric field since those can increase the effective interlayer hopping, intralayer CDW, or interlayer charge imbalance. However, simply applying these external perturbations cannot open a large gap in

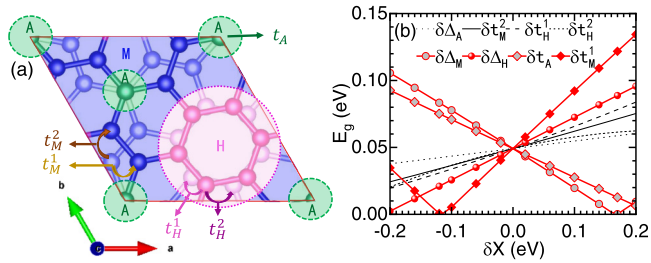

FIG. 5. (a) Three distinct regions, namely, A (green) region, M (blue) region, and H (pink) region in the moiŕe supercell. (b) The gaps as functions of the deviations of interlayer hoppings and on-site potentials δX, including δt_A, δt_M^1, δt_M^2, δt_H^1, δt_H^2, $\delta\Delta_A$, $\delta\Delta_M$, and $\delta\Delta_H$ as described in Eq. (4), which are used to simulate the effect of external perturbations. The gap at $\delta X = 0$ corresponds to the gap of $d = 2.7$ and $a = 1.42$ Å.

the system. Fortunately, the effective interlayer hopping and intralayer CDW depend on various interlayer hybridizations and intralayer on-site potentials in different regions of the supercell [see Fig. 5(a)], respectively, which provides additional degrees of freedom to tune the gap. Therefore, in the following, we will demonstrate how to open a larger gap by tuning interlayer hybridizations and on-site potentials in specific regions of the moiŕe supercell.

According to the lattice structure of tBLG we studied, totally five interlayer hopping terms between neighboring sites within the same region as defined in Fig. 5(a) and three different on-site potential terms for three different regions are believed to dominate the interlayer hoppings and intralayer CDW. Thus, we introduce perturbations to these terms as shown in Sec. II. In Fig. 5(b), we present gap amplitude as functions of these perturbations at $d = 2.7$ and $a = 1.42$ Å. It is found that the gap increases dramatically as δt_M^1 and $\delta\Delta_H$ increase or δt_A and $\delta\Delta_M$ decrease. Therefore, to open a larger gap in this system experimentally, one needs to enhance t_M^1 and Δ_H, meanwhile weaken t_A and Δ_H. Since above DFT calculations demonstrate that effective interlayer hopping dominates the gap opening, we would like to propose that applying a periodic transverse inhomogeneous pressure which affect t_M^1 and t_A in the opposite direction may be a promising way to obtain a large gap.

Finally, we will verify above proposal by first-principle calculations. In Fig. 6(a), it is shown that both t_M^1 and t_A increase with a decrease inf d, indicating that, by enlarging the interlayer distance of A region d_A and compressing that of M region d_M as shown by the colored arrow in Fig. 6(a), one may fulfill the requirement of increasing t_M^1 and decreasing t_A simultaneously. To demonstrate this, we perform DFT calculations on tBLG with region-dependent interlayer distances of $d_A = 2.7$ Å$+\Delta d$, $d_M = 2.7$ Å$-\Delta d$, and $d_H = 2.7$ Å, which can be effectively viewed as applying a periodic transverse homogeneous pressures. Figure 6(b) presents the gap as a function of Δd. It is found that the gap is larger than 100 meV when $\Delta d \geqslant 0.05$ Å. Interestingly, the band structure still satisfies the nearly linear low-energy spectra as illustrated in Fig. 6(c). The gap is of 150.1 meV when $\Delta d = 0.1$ Å, which is further confirmed by the DOS in Fig. 6(d). Therefore, a periodic transverse inhomogeneous pressure is an efficient way to open a larger gap in this system.

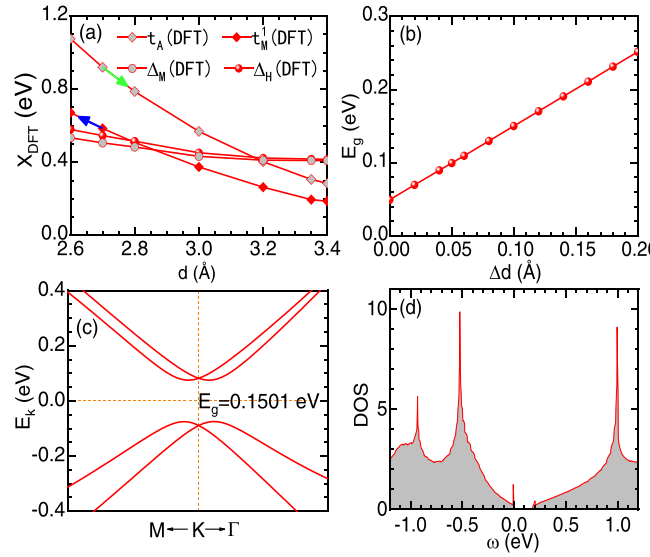

FIG. 6. (a) The DFT values of t_A, t_M^1, Δ_M, and Δ_H as functions of d. (b) The gap as a function of the height difference between A and M regions within the same layer Δd where interlayer distances of $d_A = 2.7$ Å$+\Delta d$, $d_M = 2.7$ Å$-\Delta d$, and $d_H = 2.7$ Å are used. (c) and (d) illustrate the band structure and density of state of the case $\Delta d = 0.1$ Å, respectively.

IV. DISCUSSION

Here, combining first-principle calculations with tight-binding calculations, we point out a way to open a large gap in tBLG with twisted angle $\theta = 38.21°$. All of our calculations are performed without the consideration of spin polarization since the DOS of this system near the Fermi surface is too small to stabilize a magnetic ground state. When the twisted angle is not so large, tBLG under a large transverse pressure will favor a correlated ferromagnetic ground state due to the occurrence of the flat bands [27]. However, flat bands do not exist in our case.

Our paper mainly focuses on the tBLG with twisted angle $\theta = 38.21°$. To our knowledge, the properties of tBLG are strongly dependent on the twisted angle between two layers based on model analyses. The low-energy spectra are quite different for SE-even tBLG and SE-odd tBLG where the former is gapped whereas the latter is gapless due to symmetry [41]. Although an in-plane shift of one layer with respect to the other may turn SE-even tBLG into SE-odd tBLG resulting in a gap close, SE-even tBLG is stable and can be realized in experiment [29]. We have also performed calculations on tBLG with twisted angle $\theta = 46.83°$. It is found that the gap also increases quickly when applying a transverse homogeneous pressure as illustrated in Fig. 9 of Appendix C. Thus, it is interesting to study the properties of tBLGs with other twisted angles based on first-principle calculations. However, it is beyond the scope of the present paper.

Interestingly, we have proposed here that there is an intrinsic intralayer CDW in SE-even tBLG with a large twisted angle, which has not yet been mentioned. In fact, the intralayer on-site potential differences affect mainly the low-energy spectra of tBLG as shown in Fig. 7 of Appendix A and Fig. 8 of Appendix B. However, the intralayer on-site

potential differences are neglected in long-wavelength theory [14] and tight-binding approximation [16]. As a result, flat bands with broken electron-hole symmetry, which are different from that obtained by tight-binding approximation, are observed by DFT calculations [27]. Therefore, we strongly suggest that it is necessary to include the effect of intralayer CDW in long-wavelength theory and tight-binding approximation to study the low-energy properties of tBLG.

We have shown that applying a periodic transverse inhomogeneous pressure leads to region-dependent interlayer distances and, consequently, enhance the gap. Perhaps this is not difficult to achieve in experiments. It has been observed that deposition of C_{60} on tBLG can increase the gap of tBLG from 35 to 80 meV due to the increased concentration of interayer C-C bonding [42]. Moreover, we would like to propose that deposition of polar molecule may lead to region-dependent on-site potentials which may favor a gapped state. It is worth noting that not only does the tBLG we studied open a large band gap under a periodic transverse inhomogeneous pressure, but also it still maintains nearly linear dispersion of low-energy spectra, indicating the high electron mobility still remains.

It is worth mentioning that the band gaps of semiconductors are systematically underestimated by DFT calculatons [43]. Thus, the actual band gap given by experiment may be larger than the calculated one in tBLG.

V. CONCLUSION

At large commensurate angles, tBLG which holds even parity under sublattice exchange exhibits a tiny gap. Here, we point out a way to tune this tiny gap into a larger gap. First, from first-principles calculations, we find that the gap size increases with increasing transverse homogeneous pressures, in-plane biaxial tensile strains, or transverse electric fields. We reveal that enhancement of the gap by pressures or strains is attributed to the increases in both intralayer CDW and effective interlayer hopping, whereas it is due to the formation of an interlayer charge imbalance under applied electric fields. Then, using a tight-binding model, we demonstrate how to open a larger gap by tuning interlayer hoppings and on-site potentials in specific regions of the moiŕe supercell. Finally, based on the guidance of tight-binding calculations, we propose that a periodic transverse inhomogeneous pressure can open a gap of over 100 meV, which is further confirmed by first-principle calculations. Our results provide a theoretical guidance for experiments to open a large gap in tBLG, and may pave a way for carbon-based electronics.

ACKNOWLEDGMENTS

This work was supported by the National Natural Science Foundation of China (Grants No. 11774258 and No. 12004283) and the Shanghai Science and Technology Program (Grant No. 21JC1405700).

APPENDIX A: THE t_{eff} FOR STRUCTURES WITH DIFFERENT ds

Figure 7 shows the band structures of tBLG with and without the effect of intralayer CDW for structures with different ds where the effective interlayer hopping t_{eff} for different ds are given. As can be seen, t_{eff} increases monotonously with the decrease in d.

APPENDIX B: THE t_{eff} FOR STRUCTURES WITH DIFFERENT as

Figure 8 shows the band structures of tBLG with and without the effect of intralayer CDW for structures with different as where the effective interlayer hopping t_{eff} for

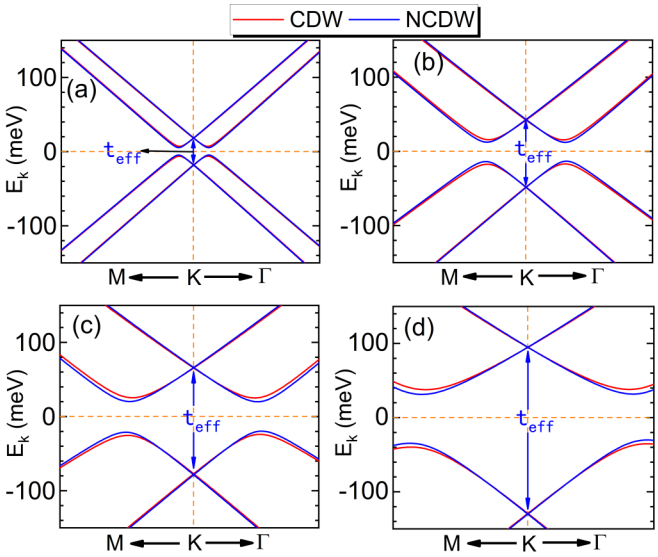

FIG. 7. At twisted angle $\theta = 38.21^\circ$, band structures of tBLG with and without the effect of intralayer CDW for different ds, $d = 3.35$, $d = 2.8$, $d = 2.7$, and $d = 2.6$ Å are used in (a)–(d) respectively. $a = 1.42$ Å is adopted in all cases.

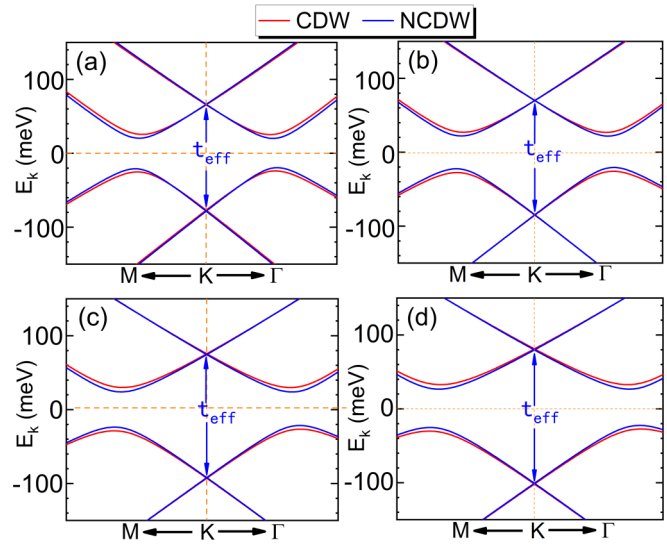

FIG. 8. At twisted angle $\theta = 38.21^\circ$, band structures of tBLG with and without the effect of intralayer CDW for different as, $a = 1.42$, $a = 1.44$, $a = 1.46$, and $a = 1.48$ Å are used in (a)–(d), respectively. $d = 2.7$ Å is adopted in all cases.

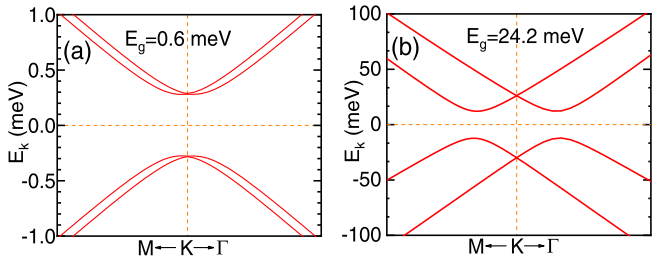

FIG. 9. Band structure of tBLG with twisted angle $\theta = 46.83°$, $d = 3.35$ and $d = 2.7$ Å are used in (a) and (b), respectively, where $a = 1.42$ Å is used.

different as are also given. It is to easy find that t_{eff} increases monotonously with the increase in a.

APPENDIX C: TUNABLE GAP IN TBLG WITH TWISTED ANGLE $\theta = 46.83°$

Figure 9 shows the band structures of tBLG with twisted angle $\theta = 46.83°$. When without a transverse homogeneous pressure ($d = 3.35$ Å) as can be seen in Fig. 9(a), the gap of the system $E_g = 0.6$ meV. The gap increases quickly under a transverse homogeneous pressure ($d = 2.7$ Å) where the system is gapped with a gap of 24.2 meV in Fig. 9(b).

[1] A. V. Rozhkov, A. O. Sboychakov, A. L. Rakhmanov, and F. Nori, Electronic properties of graphene-based bilayer systems, Phys. Rep. **648**, 1 (2016).

[2] T. Ohta, J. T. Robinson, P. J. Feibelman, A. Bostwick, E. Rotenberg, and T. E. Beechem, Evidence for Interlayer Coupling and Moiré Periodic Potentials in Twisted Bilayer Graphene, Phys. Rev. Lett. **109**, 186807 (2012).

[3] Y. Cao, V. Fatemi, A. Demir, S. Fang, S. L. Tomarken, J. Y. Luo, J. D. Sanchez-Yamagishi, K. Watanabe, T. Taniguchi, E. Kaxiras *et al.*, Correlated insulator behaviour at half-filling in magic-angle graphene superlattices, Nature (London) **556**, 80 (2018).

[4] H. C. Po, L. Zou, A. Vishwanath, and T. Senthil, Origin of Mott Insulating Behavior and Superconductivity in Twisted Bilayer Graphene, Phys. Rev. X **8**, 031089 (2018).

[5] Y. Cao, V. Fatemi, S. Fang, K. Watanabe, T. Taniguchi, E. Kaxiras, and P. Jarillo-Herrero, Unconventional superconductivity in magic-angle graphene superlattices, Nature (London) **556**, 43 (2018).

[6] X. Lu, P. Stepanov, W. Yang, M. Xie, M. A. Aamir, I. Das, C. Urgell, K. Watanabe, T. Taniguchi, G. Zhang *et al.*, Superconductors, orbital magnets and correlated states in magic-angle bilayer graphene, Nature (London) **574**, 653 (2019).

[7] L. Balents, C. R. Dean, D. K. Efetov, and A. F. Young, Superconductivity and strong correlations in moiré flat bands, Nat. Phys. **16**, 725 (2020).

[8] M. J. Park, Y. Kim, G. Y. Cho, and SungBin Lee, Higher-Order Topological Insulator in Twisted Bilayer Graphene, Phys. Rev. Lett. **123**, 216803 (2019).

[9] M. Kindermann, Topological Crystalline Insulator Phase in Graphene Multilayers, Phys. Rev. Lett. **114**, 226802 (2015).

[10] M. Sprinkle, D. Siegel, Y. Hu, J Hicks, A. Tejeda, A. Taleb-Ibrahimi, P. Le Fèvre, F. Bertran, S. Vizzini, H. Enriquez, S. Chiang, P. Soukiassian, C. Berger, W. A. de Heer, A. Lanzara, and E. H. Conrad, First Direct Observation of a Nearly Ideal Graphene Band Structure, Phys. Rev. Lett. **103**, 226803 (2009).

[11] S. Shallcross, S. Sharma, and O. A. Pankratov, Quantum Interference at the Twist Boundary in Graphene, Phys. Rev. Lett. **101**, 056803 (2008).

[12] S. Shallcross, S. Sharma, E. Kandelaki, and O. A. Pankratov, Electronic structure of turbostratic graphene, Phys. Rev. B **81**, 165105 (2010).

[13] J. B. Oostinga, H. B. Heersche, X. Liu, A. F. Morpurgo, and L. M. K. Vandersypen, Gate-induced insulating state in bilayer graphene devices, Nat. Mater. **7**, 151 (2008).

[14] E. J. Mele, Commensuration and interlayer coherence in twisted bilayer graphene, Phys. Rev. B **81**, 161405(R) (2010).

[15] E. J. Mele, Interlayer coupling in rotationally faulted multilayer graphenes, J. Phys. D: Appl. Phys. **45**, 154004 (2012).

[16] A. O. Sboychakov, A. L. Rakhmanov, A. V. Rozhkov, and F. Nori, Electronic spectrum of twisted bilayer graphene, Phys. Rev. B **92**, 075402 (2015).

[17] Z. Khatibi, A. Namiranian, and F. Parhizgar, Strain impacts on commensurate bilayer graphene superlattices: Distorted trigonal warping, emergence of bandgap and direct-indirect bandgap transition, Diam. Relat. Mater. **92**, 228 (2019).

[18] A. V. Rozhkov, A. O. Sboychakov, A. L. Rakhmanov, and F. Nori, Single-electron gap in the spectrum of twisted bilayer graphene, Phys. Rev. B **95**, 045119 (2017).

[19] Y. Cao, J. Y. Luo, V. Fatemi, S. Fang, J. D. Sanchez-Yamagishi, K. Watanabe, T. Taniguchi, E. Kaxiras, and P. Jarillo-Herrero, Superlattice-Induced Insulating States and Valley-Protected Orbits in Twisted Bilayer Graphene, Phys. Rev. Lett. **117**, 116804 (2016).

[20] K. Kim, M. Yankowitz, B. Fallahazad, S. Kang, H. C. P. Movva, S. Huang, S. Larentis, C. M. Corbet, T. Taniguchi, K. Watanabe *et al.*, van der waals heterostructures with high accuracy rotational alignment, Nano Lett. **16**, 1989 (2016).

[21] K. Kim, A. DaSilva, S. Huang, B. Fallahazad, S. Larentis, T. Taniguchi, K. Watanabe, B. J. LeRoy, A. H. MacDonald, and E. Tutuc, Tunable moiré bands and strong correlations in small-twist-angle bilayer graphene, Proc. Natl. Acad. Sci. USA **114**, 3364 (2017).

[22] Y. X. Zhao and I. L. Spain, X-ray diffraction data for graphite to 20 GPa, Phys. Rev. B **40**, 993 (1989).

[23] K. Cao, S. Feng, Y. Han, L. Gao, T. H. Ly, Z. Xu, and Y. Lu, Elastic straining of free-standing monolayer graphene, Nat. Commun. **11**, 284 (2020).

[24] J.-B. Liu, P.-J. Li, Y.-F. Chen, Z.-G. Wang, F. Qi, J.-R. He, B.-J. Zheng, J.-H. Zhou, W.-L. Zhang, L. Gu, and Y.-R. Li, Observation of tunable electrical bandgap in large-area twisted bilayer graphene synthesized by chemical vapor deposition, Sci. Rep. **5**, 15285 (2015).

[25] S. Carr, S. Fang, P. Jarillo-Herrero, and E. Kaxiras, Pressure dependence of the magic twist angle in graphene superlattices, Phys. Rev. B **98**, 085144 (2018).
[26] L. Ge, K. Ni, X. Wu, Z. Fu, Y. Lu, and Y. Zhu, Emerging flat bands in large-angle twisted bi-layer graphene under pressure, Nanoscale **13**, 9264 (2021).
[27] F. Yndurain, Pressure-induced magnetism in rotated graphene bilayers, Phys. Rev. B **99**, 045423 (2019).
[28] N. V. Tepliakov, Q. Wu, and O. V. Yazyev, Crystal field effect and electric field screening in multilayer graphene with and without twist, Nano Lett. **21**, 4636 (2021).
[29] E. Koren, I. Leven, E. Lörtscher, A. Knoll, O. Hod, and U. Duerig, Coherent commensurate electronic states at the interface between misoriented graphene layers, Nat. Nanotechnol. **11**, 752 (2016).
[30] P. E. Blöchl, Projector augmented-wave method, Phys. Rev. B **50**, 17953 (1994).
[31] G. Kresse and J. Furthmüller, Efficient iterative schemes for ab initio total-energy calculations using a plane-wave basis set, Phys. Rev. B **54**, 11169 (1996).
[32] G. Kresse and J. Furthmüller, Efficiency of ab-initio total energy calculations for metals and semiconductors using a plane-wave basis set, Comput. Mater. Sci. **6**, 15 (1996).
[33] J. P. Perdew, K. Burke, and M. Ernzerhof, Generalized Gradient Approximation Made Simple, Phys. Rev. Lett. **77**, 3865 (1996).
[34] K. Lee, É. D. Murray, L. Kong, B. I. Lundqvist, and D. C. Langreth, Higher-accuracy van der waals density functional, Phys. Rev. B **82**, 081101(R) (2010).
[35] I. Hamada, van der waals density functional made accurate, Phys. Rev. B **89**, 121103(R) (2014).
[36] R. R. Del Grande, M. G. Menezes, and R. B. Capaz, Layer breathing and shear modes in multilayer graphene: a dft-vdw study, J. Phys.: Condens. Matter **31**, 295301 (2019).
[37] N. Marzari, A. A. Mostofi, J. R. Yates, I. Souza, and D. Vanderbilt, Maximally localized wannier functions: Theory and applications, Rev. Mod. Phys. **84**, 1419 (2012).
[38] A. A. Mostofi, J. R. Yates, Y.-S. Lee, I. Souza, D. Vanderbilt, and N. Marzari, Wannier90: A tool for obtaining maximally-localised wannier functions, Comput. Phys. Commun. **178**, 685 (2008).
[39] A. O. Sboychakov, A. V. Rozhkov, A. L. Rakhmanov, and F. Nori, Externally Controlled Magnetism and Band Gap in Twisted Bilayer Graphene, Phys. Rev. Lett. **120**, 266402 (2018).
[40] J. M. B. Lopes Dos Santos, N. M. R. Peres, and A. H. Castro Neto, Graphene Bilayer with a Twist: Electronic Structure, Phys. Rev. Lett. **99**, 256802 (2007).
[41] E. J. Mele, Band symmetries and singularities in twisted multilayer graphene, Phys. Rev. B **84**, 235439 (2011).
[42] J. Park, W. C. Mitchel, S. Elhamri, L. Grazulis, J. Hoelscher, K. Mahalingam, C. Hwang, S.-K. Mo, and J. Lee, Observation of the intrinsic bandgap behaviour in as-grown epitaxial twisted graphene, Nat. Commun. **6**, 5677 (2015).
[43] F. Aryasetiawan and O. Gunnarsson, The GW method, Rep. Prog. Phys. **61**, 237 (1998).